Visualizing In-Organ Tumors in Augmented Monocular Laparoscopy

Erol Özgür   Alexis Lafont   Adrien Bartoli

EnCoV, IP, UMR 6602 CNRS, Université Clermont Auvergne, SIGMA, France

ABSTRACT

One of the important goals of medical augmented reality is to reveal the hidden anatomy, such as a tumor in an organ. However, conveying a hidden tumor's depth to the user effortlessly and precisely is still an unsolved problem. This is especially difficult in monocular laparoscopy. First, the number of available depth cues is in practice limited to only two: occlusion and relative size. Second, exploiting these cues is not an easy task either. We propose a specific visualization consisting of auxiliary orthographic tumor silhouettes on the front and back surfaces of the organ and a semi-transparent tumor in between. This creates two depth planes forming a perceivable ratio-scaled metric space for the tumor. We conducted a user study to evaluate the proposed visualization. The results show that sub-surface tumor depth perception is improved dramatically compared to the conventional transparent overlay.

1 INTRODUCTION

Augmented Reality (AR) plays an increasingly important role in medicine [25]. It may become especially important in laparoscopy (see figure 1), which still challenges surgeons in some procedures, such as the tumorectomies. Tumorectomy is the surgical removal of a tumor with a minimal amount of healthy tissue from the host organ. Laparoscopic tumorectomy may be difficult when the tumor
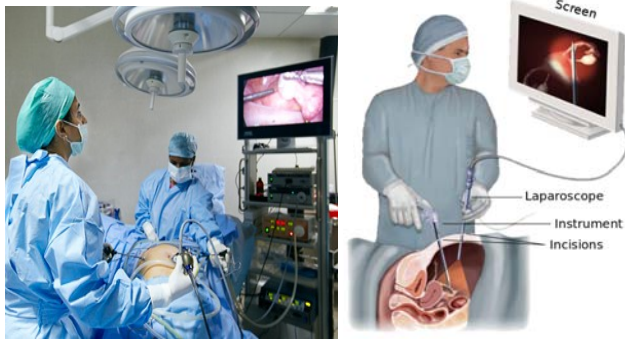

Figure 1: In laparoscopy, surgeons watch a 2D screen displaying the patient's abdominal cavity filmed by a laparoscope, inserted in an incision of about one centimeter. They manipulate the organ with surgical instruments inserted through similar incisions.

is hidden in the organ, because there is currently no means to localize it. In particular, there is no tactile feedback. AR can help surgeons by augmenting the tumor, available from preoperative CT or MR volumes, on the live laparoscopy video. It can be implemented without additional hardware. In order to achieve this, one must solve two difficult problems: *registration between the preoperative volume and the laparoscope's image* and *occluded object*

---

e-mail: erol.ozgur@uca.fr, alexis.lafont@uca.fr, adrien.bartoli@gmail.com

visualization. The medical AR literature mostly concentrates on the registration problem [8, 7, 6, 20, 21, 22, 14, 3, 23]. For instance, [14, 3, 23] worked on registration for the liver. Both [23] and [14] achieve deformable registration from multiple images using contours, while [3] rigidly registers an intraoperative CT to a laparoscopy image using shading. [8, 7] worked on the uterus and achieve rigid registration from multiple images using the silhouette.

Given a registration solution, we focus on hidden anatomy visualization in monocular laparoscopy. For instance, this may help a surgeon to plan an optimal resection corridor towards a tumor and reduce damage in the healthy tissue. However, it is unnatural for the human eye to see through an opaque surface. Conveying a precise and effortless depth perception to a surgeon for a hidden part of the anatomy is thus a challenging task. Few methods have so far been proposed for the medical AR visualization of the hidden anatomical structures [27, 16, 24]. None of the existing methods form a satisfying solution to visualize the hidden anatomy in monocular laparoscopy. We propose a new visualization specifically designed for in-organ tumors. A user study confirmed that this new visualization improves depth perception of in-organ tumors dramatically compared to the conventional transparent overlay visualization.

2 AUGMENTED REALITY FOR HIDDEN STRUCTURES

Most of the literature in depth perception for X-Ray AR focused on mobile hand-held displays and head-mounted displays (HMD) [1, 2, 5, 11, 17, 24, 4, 10]. These platforms allow one to use multiple depth cues (static/dynamic, monocular/stereo) to counterbalance the depth misperception of occluded object visualization. In monocular laparoscopy however, one must use monocular X-Ray AR. Occlusion is then known to be the most powerful depth cue [9]. In this case, occluded object visualization becomes self-conflicting, because the occluded tumor is rendered onto its occluding organ, and thus occludes the occluding surface. Consequently, the surgeon's visual perception stimulates the occlusion message: "the rendered tumor occludes the organ". This makes the surgeon see the rendered tumor as if floating on top of its occluding surface [2]. To fix this misperception, a *virtual window* was introduced on the occluding surface [2]. This fakes the surgeon's visual perception by giving the impression of seeing the other side of the occluding surface. However, it was reported that the rendered tumor continues to float even under motion [12], until some occlusion also happens in the virtual window [5].

3 WHICH DEPTH CUES TO USE IN LAPAROSCOPY?

We research a solution applicable to the de facto laparoscopy setup. This is for two reasons. First, a solution should be usable directly in the operating room (OR) by installing only an AR software. Second, the surgeons do prefer not to wear a Head Mounted Display, because of quick fatigue and sterility. We are thus constrained to use a regular screen (a fixed monocular, flat non-3D display). The screen cannot be aligned between the surgeon and the patient to provide a see-through effect which would improve both AR immersion and surgeon's hand-eye coordination. Consequently, we can only use the monocular depth cues. Figure 2 shows the strength of the most important monocular depth cues versus their effective ranges. The strength of the cues is expressed in depth contrast. A depth contrast is computed as the difference in depth of two objects
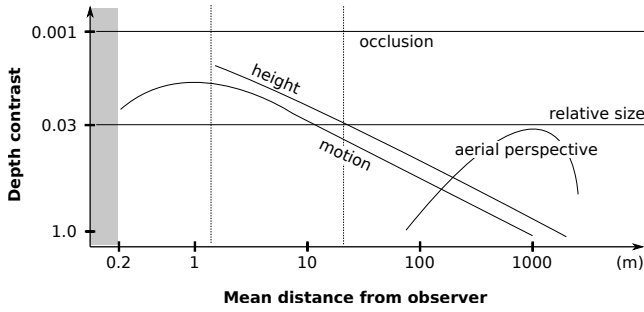
Figure 2: Monocular depth cues and laparoscopy's work depth range (shaded area). The smaller the depth contrast, the stronger the cue. Graphics adapted from [9].

divided by the mean distance of these objects from the observer. It states that a small depth difference is negligible if the mean distance is high, while the same small depth difference matters if the mean distance is low.

We now discuss the availability of these depth cues in laparoscopy. The laparoscope has a very small work range ($10\,cm$ to $20\,cm$). Most cues' effective range fall off this work range. Laparoscopy images are sharp everywhere because the laparoscope's depth of field (effective focus range) covers all of its work range. This eliminates the aerial perspective and texture gradient cues. The linear perspective cue does not exist either because of the curvilinear anatomical shapes and the distortion in the wide-angle optics of the laparoscope. A consistent shading cue can be implemented easily since the light source's position is known. It is a rather strong cue on shape perception, but weak on depth perception of disjoint surfaces. A consistent shadow cue is useless because a virtual object's shadow would be occluded by itself since the light source and the camera's origin are collocated at the laparoscope's distal end. Finally, during organ resection, the laparoscope is focused on the area of resection for the surgeon to operate stably and safely. More explicitly, a hand-held laparoscope tries to keep the resection area in the center of the image by generally moving slowly, or rapidly at times. This practically eliminates the motion depth cue. Consequently, we are left with only the occlusion and relative size depth cues to correct depth misperception for occluded object visualization.

4 PROPOSED VISUALIZATION

We now work under the premises that occlusion and relative size form the strongest depth cues for monocular laparoscopy. Occlusions convey an ordinal depth and are effective at any distance. However they cannot be used directly for a tumor completely occluded by the organ. We thus need something similar to the proven-concept of "virtual window with some occlusion" visualization so that the occluded tumor can be augmented with least misperception. It was shown that the virtual window improves depth perception when the occluding surface's context features (e.g., edges, texture) are preserved inside the window in order to generate some occlusion on the augmented object [1, 13, 15]. Lerotic et al. used a similar idea in lung laparoscopy by overlaying accentuated surface ridges onto the augmented tumor [19]. However, an organ's visible surface might not always have easily detectable context features. Many organs such as the uterus, the kidney and the liver contain smooth regions with an homogeneous appearance. If the laparoscope views such a region, then some visualization approaches such as the transparent overlay and the ghosting method would fail. Some such as the virtual window and the random-dot mask would succeed but would occlude a relatively large part of the laparoscopy image [27]. A ghosting method with synthetic features would also

succeed [29] but would require changing the organ's appearance, which is not desirable in laparoscopy. A solution for this would be to use auxiliary occluded augmentations of the object of interest [17, 18]. It is however not very intuitive to add another copy of the tumor inside the organ. This is for two reasons. First, this might confuse the surgeon. Second, this clutters the scene since the field of view is small, and we want to keep the original laparoscopy image as clean as possible.

Our visualization replaces the virtual window placed on the organ's occluding front surface with the tumor's silhouette. We also place a second silhouette on the back surface of the organ. Both silhouettes are obtained by orthographic projection along the sight-line passing through the tumor's center of mass (see figure 3). The silhouettes obtained by orthographic projection thus become the auxiliary augmentations at the exact size of the tumor. Such auxiliary augmentations should have at least one dimension to be the same as the occluded object so that the relative size depth cue can be enabled for use [17]. Consequently, the silhouettes form a perceivable ratio-scaled metric space for the tumor between the front and back surfaces of the organ.

We also lower the luminance contrast between the rendered tumor and its surrounding region visible through the front silhouette by adding a virtual transparent dark screen in the form of the front silhouette. This should allow the tumor to be perceived deeper than it is [26], and thus help suppressing the floating on organ effect. Intuitively, the inner space of the organ should be seen darker (assuming that it receives less light) than its outer visible surface. This virtual dark screen thus also gives the feeling of seeing inside of the organ through the front silhouette by imitating the darkness of the inner space.

We finally render the tumor as a transparent surface on the surgical video. Transparency yields the impression of seeing the occluding surface's context features overlaid on the augmented tumor. We thus do not need to detect any context features. Consequently, some spontaneous occlusion is generated for better depth perception. Importantly, in the proposed visualization, the tumor is always fully perceivable.

5 AUGMENTATION MODELING

Let $\boldsymbol{\ell} \subset \mathbb{R}^3$ be the sight-line passing through the tumor's center of mass, $S \subset \mathbb{R}^3$ be the organ's surface and $T \subset \mathbb{R}^3$ be the tumor's surface. We compute the intersection points as $\{\mathbf{x}_{front}, \mathbf{x}_{back}\} = \boldsymbol{\ell} \cap S$. We then define the front projection plane π_{front} and back projection plane π_{back} at the intersection points with normals aligned with the sight-line $\boldsymbol{\ell}$. Let also $\Pi : \mathbb{R}^3 \to \mathbb{R}^2$, $\phi : \mathbb{R}^2 \to \mathbb{R}^2$, $\mathbf{O}_{front} : \mathbb{R}^3 \to \pi_{front}$ and $\mathbf{O}_{back} : \mathbb{R}^3 \to \pi_{back}$ be, respectively, the perspective projection function onto the image, the silhouette extraction function and the orthographic projection functions onto the front and back planes. We compute the tumor's silhouette curves as follows:

$$s_f = \Pi(\phi(\mathbf{O}_{front}(T))) \quad (1)$$
$$s_b = \Pi(\phi(\mathbf{O}_{back}(T))) \quad (2)$$

where $s_f \subset \mathbb{R}^2$ is the front silhouette curve and $s_b \subset \mathbb{R}^2$ is the back silhouette curve. We finally obtain the augmented image I_A as in the BLEND procedure given in figure 5. In the BLEND procedure, $\alpha_f, \alpha_{\overline{m}}, \alpha_t, \alpha_b \in [0,1]$ are the adjustable transparency coefficients, An $\alpha = 1$ implies 100% opaqueness and respectively an $\alpha = 0$ implies 100% transparency. We ordered the transparency coefficients as $1 \geqslant \alpha_f \geqslant \alpha_b > \alpha_t > 0$ and $1 > \alpha_{\overline{m}} \geqslant \alpha_t$. In the BLEND procedure, line 01 creates a binary mask image M from the front silhouette curve s_f with zeros inside the silhouette and ones outside. Line 02 generates a new binary mask image $\overline{M}$ by inverting M. Lines 03 and 04 generate images of the silhouette curves with the desired thicknesses and colors. The front silhouette is made twice as thick than the back one in order to simulate a relative size
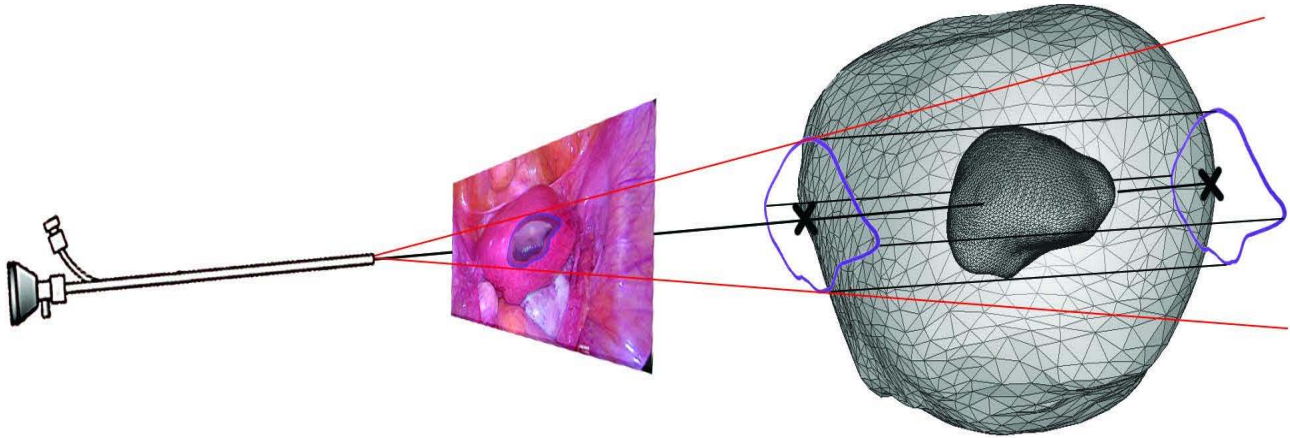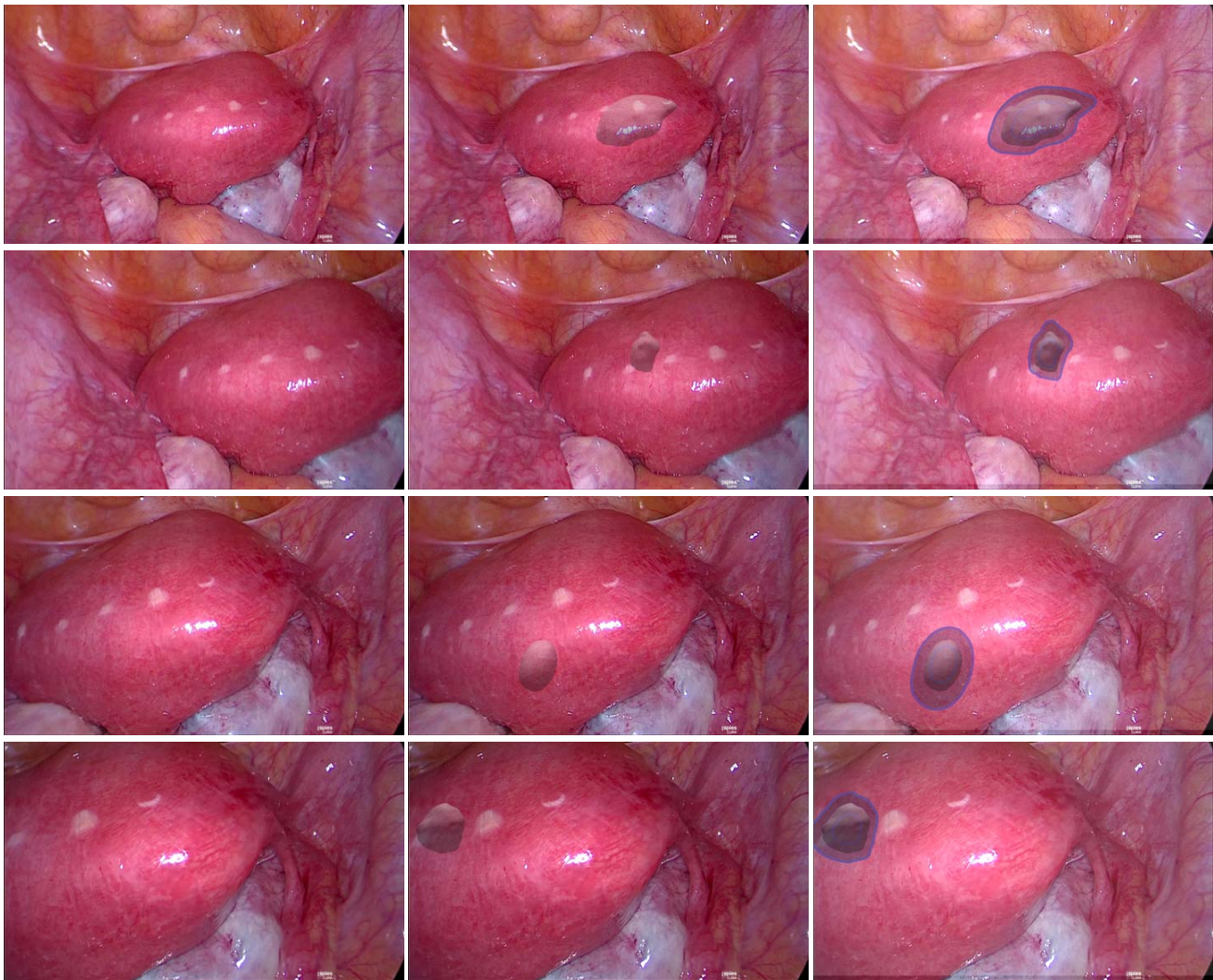
Figure 3: Proposed in-organ tumor visualization. The silhouettes are obtained by orthographic projection onto the front and back planes. The planes' orientations are defined from the sight-line passing through the tumor's center of mass. The planes are located at the intersection points of the organ's surface with this sight-line.

(a) Original laparoscopy images   (b) Transparent overlays   (c) Proposed visualizations

Figure 4: Augmentation examples of in-organ uterus tumors.

Procedure: BLEND
Inputs: Laparoscopy image I, curves s_f and s_b and tumor T
Output: Augmented image I_A

01:   $M = $ `maskFromCurve`(s_f)

02:   $\overline{M} = $ `invertMask`(M)

03:   $I_f = $ `imageFromCurve`$(s_f, 2*$`thickness`$, $`color1`$)$

04:   $I_b = $ `imageFromCurve`$(s_b, $`thickness`$, $`color1`$)$

05:   $I_t = $ `render`$(\Pi, T, $`shading`$, $`color2`$)$

06:   $I_A = M \cdot I + \alpha_{\overline{m}}\, \overline{M} \cdot I$

07:   **for** $i \in \{b, t, f\}$

08:     **for** $x = 1 \dots$ `width`(I), $y = 1 \dots$ `height`(I)

09:       **if** $I_i(x,y) \neq \mathbf{0}$ **then** $I_A(x,y) = \alpha_i\, I_i(x,y) + (1-\alpha_i)\, I_A(x,y)$

10:     **end**

11:   **end**

Figure 5: Blending for the proposed visualization.

depth cue and intensify a correct ordinal depth perception among them. We chose the thickness values empirically with regard to the size of the input laparoscopy image I which is 1920×1080 pixels. The silhouettes' colors are set to the same value and chosen empirically with regard to the input laparoscopy image's pixel intensities. Line 05 renders the tumor with the desired shading model and color. We used the Lambertian shading model for the tumor. The tumor's color is again chosen empirically. Line 06 forms the virtual dark screen in the form of the front silhouette. Finally, lines 07-11 blend linearly the back silhouette, the tumor and the front silhouette progressively. The full augmentation, including equations (1) and (2), was implemented in C++ using the OpenGL and OpenCV libraries. The augmentation implementation does not require any specific hardware and runs very fast even on a standard personal computer.

6 USER STUDY DESIGN AND RESULTS

We conducted a user study to compare our proposed visualization against the conventional transparent overlay visualization. We used a patient's uterus for the tumor augmentation. The laparoscopy images were captured using a 10mm Karl Storz zero-degree HD laparoscope with CLARA image enhancement. The images are 1920×1080 pixels. The uterus' preoperative MR volume was registered to the laparoscopy images using [7]. The registration method [7] works in realtime (~ 25 fps). It is implemented in C++ and CUDA, and runs on a standard Intel i7 desktop PC with an NVidia GTX 660 CUDA-enabled graphics card. We set the transparency coefficients as $\alpha_f = 0.45$, $\alpha_{\overline{m}} = 0.65$, $\alpha_t = 0.35$, $\alpha_b = 0.45$ in the proposed visualization, and $\alpha_t = 0.35$ in the conventional transparent overlay visualization.

6.1 Cases Generation

We selected four different laparoscopy images of the uterus for the user study. We used four uterine tumors with different sizes and locations for each image. This thus yielded 16 different cases to evaluate. The uterine tumors were segmented with the MITK software [28] from different patients' preoperative MRI and were thus realistic regarding their shapes and locations. Figure 4 shows visualization examples.

6.2 Participants and Study Design

12 people participated to the study. Most participants never saw a uterus and tumors before. Some participants were experienced in seeing laparoscopy images. Two participants were surgeons. The study was divided into two parts. These 12 participants attended initially to the first part of the study and then to the second part of the study.

In the first part, the participants were told that *(i)* they will see images of a uterus which contains a hidden tumor, *(ii)* they have to tell if the rendered tumor is perceived inside or outside the uterus and *(iii)* they will see two different visualization approaches: the transparent overlay visualization and the proposed visualization. The participants were not told anything about the meaning of the silhouettes in the proposed visualization.

In the second part, the participants were told that *(i)* in the proposed visualization the silhouettes represent the orthographic projections of the tumor and are located on the front and back surfaces of the organ and *(ii)* they have to tell again if the rendered tumor is perceived inside or outside the uterus in the proposed visualization. In the second part, we did not show the participants the images of the transparent overlay visualization again, because there was nothing more to add as information for this visualization than the first part of the study.

6.3 Results

For the first part of the user study, we showed the participants the 16 different tumor cases with both visualizations. In figure 6, first two bars show the percentages of participants perceiving a tumor inside the uterus versus the different cases in both visualizations. We observe that the proposed visualization performs better than the conventional transparent overlay visualization, except in case 2. Figure 7 shows the images for this case. This is because the proposed visualization converges to the conventional transparent overlay visualization when a tumor is close to the visible surface. It becomes even worse than the conventional transparent overlay visualization because of the cluttering silhouettes on the surface tumor. This can be easily improved by switching back to the conventional transparent overlay visualization when a tumor is close to the visible surface.

For the second part of the user study, we re-showed the participants the different tumor cases with the proposed visualization. In figure 6, third bar shows the percentages of participants perceiving a tumor inside the uterus versus the different cases, after the participants were informed about the meaning of the silhouettes. We observe that the proposed visualization with informed participants performs better than with uninformed participants. The possible reason why informed participants performed better is that the relative size depth cue was triggered deliberately. This helped switching from perceiving tumors outside to inside almost in all cases, except case 6. This is because once again in case 6 the tumor is very close to the visible surface of the uterus and thus kept being perceived outside, similarly to case 2, as shown in figure 7.

Table 1 lists the mean and standard deviation of perceiving tumors inside the uterus (for figure 6) versus the visualization methods in two parts. We conclude from Table 1 that the proposed visualization even with uninformed participants almost doubles the quality of depth perception as compared with the conventional transparent overlay.

	Transparent overlay	Proposed visualization (uninformed)	Proposed visualization (informed)
Mean	43.75 %	77.60 %	89.06 %
SD	15.95 %	11.67 %	10.85 %

Table 1: Mean and standard deviation (SD) of perceiving tumors inside the uterus versus the visualization methods.

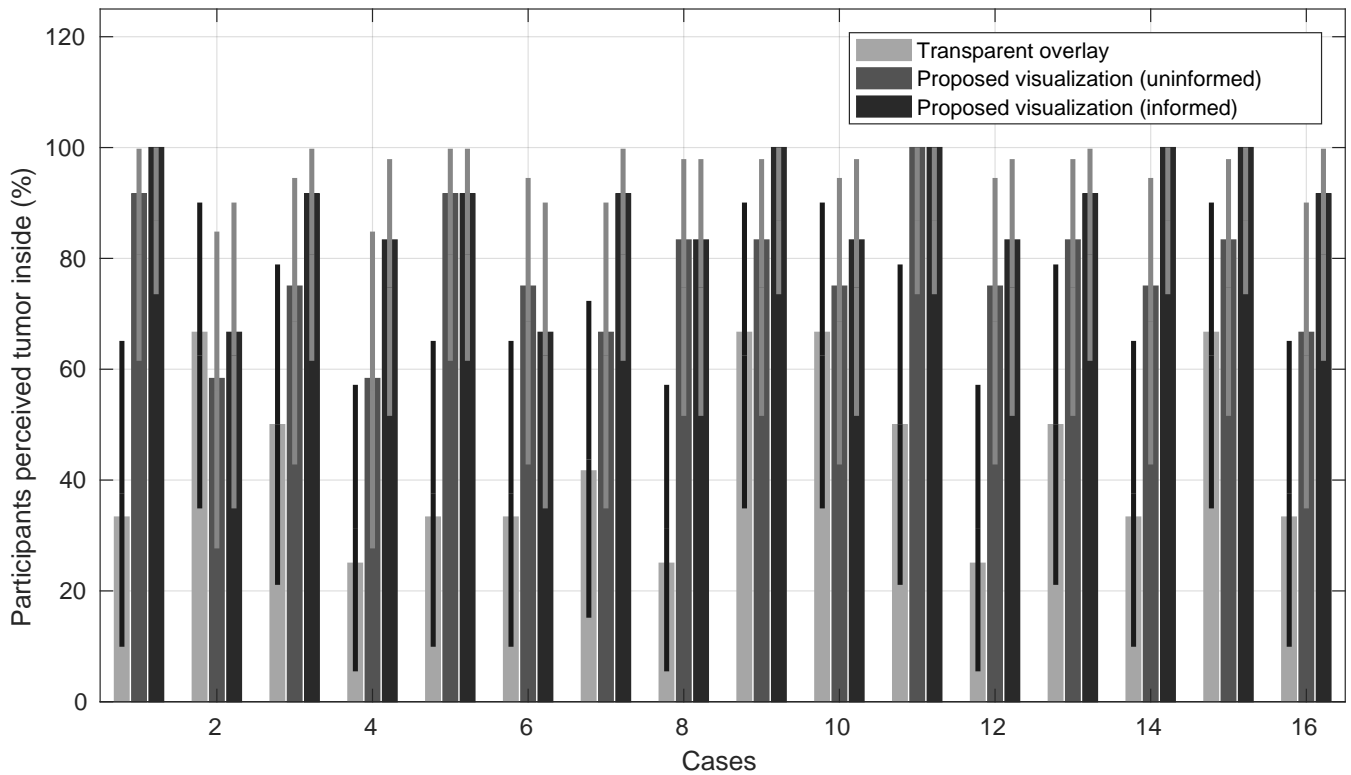We also asked each participant to guess the location of the tumor

Figure 6: User study results. The graphics show the percentages of participants perceiving a tumor inside the uterus versus the different cases. The thin bars show the 95% confidence intervals of the tumor cases for each visualization technique. Clopper-Pearson method is used to calculate confidence intervals.

in the proposed visualization by choosing one of the options: closer to the front surface, half-way or closer to the back surface. Almost all participants perceived each tumor deeper than it was. This justifies the effect of lowered luminance contrast between the rendered tumor and its surrounding region. We asked the same question with the transparent overlay visualization, and most participants could not even make a guess.

Although, we did not investigate the motion depth cue, we prepared a video of the proposed visualization under some observational motion over the uterus. The registration and tracking for this video is performed again using only the registration method [7], since it is fast enough to also replace tracking. We showed this video to the participants and asked if the motion contributed to the proposed visualization for better depth perception. The participants commented that the spontaneous occlusions (due to transparency) sliding over the tumor strengthen their perception to accept the tumor inside the uterus. We provide this video in `http://igt.ip.uca.fr/~ab`.

7 CONCLUSION

We have proposed a new in-organ tumor visualization approach for medical AR. The user study showed that it improves depth perception compared to conventional transparent overlay visualization. The proposed visualization modifies the image less than the state-of-the-art visualization approaches such as the virtual window and the random-dot mask approaches. It is also simple to implement and computationally efficient.

As future work, we shall *(i)* compare the proposed approach with the other state-of-the-art visualization approaches, *(ii)* investigate the biased depth perception in the proposed visualization using a better laparoscopic illumination model *e.g.*, light falloff, *(iii)* ex-

plore the color choice for the proposed visualization and *(vi)* test the proposed visualization in vivo.

REFERENCES

[1] B. Avery, C. Sandor, and B. H. Thomas. Improving spatial perception for augmented reality x-ray vision. *IEEE Conference on Virtual Reality*, pages 79–82, 2009.

[2] M. Bajura, H. Fuchs, and R. Ohbuchi. Merging virtual objects with the real world: Seeing ultrasound imagery within the patient. *International Conference on Computer Graphics and Interactive Techniques*, pages 203–210, 1992.

[3] S. Bernhardt, S. Nicolau, A. Bartoli, V. Agnus, L. Soler, and C. Doignon. Using shading to register an intraoperative CT scan to a laparoscopic image. *International Workshop on Computer Assisted and Robotics Endoscopy at MICCAI*, 2015.

[4] M. Berning, D. Kleinert, T. Riedel, and M. Beigl. A study of depth perception in hand-held augmented reality using autostereoscopic displays. *International Symposium on Mixed and Augmented Reality*, 2014.

[5] C. Bichlmeier, T. Sielhorst, S. Heining, and N. Navab. Improving depth perception in medical AR: A virtual vision panel to the inside of the patient. *Bildverarbeitung für die Medizin*, pages 217–221, 2007.

[6] T. Collins, A. Bartoli, N. Bourdel, and M. Canis. Dense, robust and real-time 3D tracking of deformable organs in monocular laparoscopy. *Medical Image Computing and Computer Assisted Intervention*, 2016.

[7] T. Collins, D. Pizarro, A. Bartoli, N. Bourdel, and M. Canis. Computer-aided laparoscopic myomectomy by augmenting the uterus
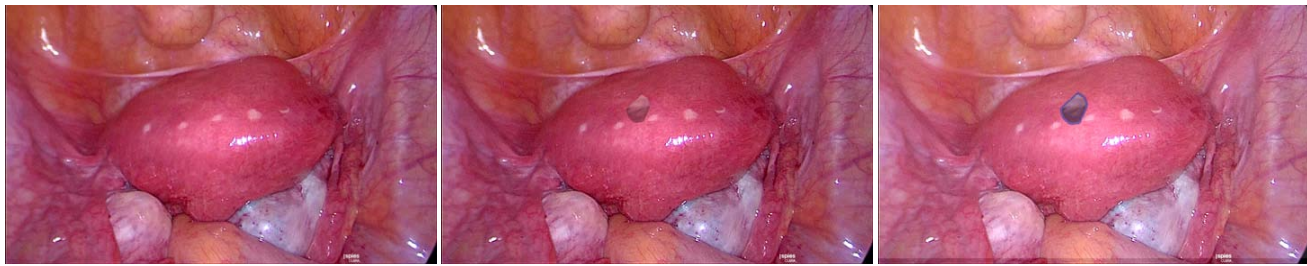
(a) Original laparoscopy image	(b) Transparent overlay	(c) Proposed visualization

Figure 7: The proposed visualization fails for tumors close to the visible surface. This is because it converges to the conventional transparent overlay and becomes even worse due to the silhouettes cluttering the rendered surface tumor. Such cases can be easily fixed by switching the proposed visualization to the conventional transparent overlay.

with pre-operative MRI data. *International Symposium on Mixed and Augmented Reality*, 2014.

[8] T. Collins, D. Pizarro, A. Bartoli, M. Canis, and N. Bourdel. Realtime wide-baseline registration of the uterus in monocular laparoscopic videos. *International Workshop on Medical Imaging and Augmented Reality at MICCAI*, 2013.

[9] J. Cutting and P. Vishton. Perceiving layout and knowing distances: The integration, relative potency, and contextual use of different information about depth. *In Perception of Space and Motion*, pages 69–117, 1995.

[10] A. Dey, A. Cunningham, and C. Sandor. Evaluating depth perception of photorealistic mixed reality visualizations for occluded objects in outdoor environments. *IEEE Symposium on 3D User Interfaces*, 2010.

[11] H. Fuchs, M. Livingston, R. Raskar, D. Colucci, K. Keller, A. State, J. Crawford, P. Rademacher, S. Drake, and A. Meyer. Augmented reality visualization for laparoscopic surgery. *Medical Image Computing and Computer Assisted Intervention*, 1998.

[12] C. Furmanski, R. Azuma, and M. Daily. Augmented-reality visualization guided by cognition: Perceptual heuristics for combining visible and obscured information. *International Symposium on Mixed and Augmented Reality*, pages 215–224, 2002.

[13] A. A. Gooch and B. Gooch. Non-photorealistic rendering. *AKPeters Ltd.*, 2001.

[14] N. Haouchine, F. Roy, L. Untereiner, and S. Cotin. Using contours as boundary conditions for elastic registration during minimally invasive hepatic surgery. *International Conference on Intelligent Robots and Systems*, 2016.

[15] D. Kalkofen, E. Mendez, and D. Schmalstieg. Comprehensible visualization for augmented reality. *IEEE Transactions on Visualization and Computer Graphics*, 15(2):193–204, 2009.

[16] M. Kersten-Oertel, I. Gerard, S. Drouin, K. Mok, D. Sirhan, D. Sinclair, and D. Collins. Augmented reality in neurovascular surgery: feasibility and first uses in the operating room. *International Journal of Computer Assisted Radiology and Surgery*, 10(11):1823–1836, 2015.

[17] M. Kyto, A. Makinen, J. Hakkinen, and P. Oittinen. Improving relative depth judgments in augmented reality with auxiliary augmentations. *ACM Transactions on Applied Perception*, 10(1):1–21, 2013.

[18] M. Kyto, A. Makinen, T. Tossavainen, and P. Oittinen. Stereoscopic depth perception in video see-through augmented reality within action space. *Journal of Electronic Imaging*, 23(1), 2014.

[19] M. Lerotic, A. Chung, G. Mylonas, and G. Yang. pq-space based non-photorealistic rendering for augmented reality. *Medical Image Computing and Computer Assisted Intervention*, 2007.

[20] L. Maier-Hein, A. Groch, A. Bartoli, S. Bodenstedt, G. Boissonnat, P. Chang, N. Clancy, D. Elson, S. Haase, E. Heim, J. Hornegger, P. Jannin, H. Kenngott, T. Kilgus, B. Müller-Stich, D. Oladokun, S. Röhl, T. dos Santos, H. Schlemmer, A. Seitel, S. Speidel, M. Wagner, and D. Stoyanov. Comparative validation of single-shot optical techniques for laparoscopic 3D surface reconstruction. *IEEE Transactions on Medical Imaging*, 33(10):1913–1930, 2014.

[21] L. Maier-Hein, P. Mountney, A. Bartoli, H. Elhawary, D. Elson, A. Groch, A. Kolb, M. Rodrigues, J. Sorger, S. Speidel, and D. Stoyanov. Optical techniques for 3D surface reconstruction in computer-assisted laparoscopic surgery. *Medical Image Analysis*, 17(8):974–996, 2013.

[22] G. Puerto-Souza, J. Cadeddu, and G. Mariottini. Toward long-term and accurate augmented-reality for monocular endoscopic videos. *IEEE Transactions on Biomedical Engineering*, 61(10):2609–2620, 2014.

[23] A. Saito, M. Nakao, Y. Uranishi, and T. Matsuda. Deformation estimation of elastic bodies using multiple silhouette images for endoscopic image augmentation. *International Symposium on Mixed and Augmented Reality*, 2015.

[24] T. Sielhorst, C. Bichlmeier, S. Heining, and N. Navab. Depth perception – a major issue in medical AR: evaluation study by twenty surgeons. *Medical Image Computing and Computer Assisted Intervention*, 2006.

[25] T. Sielhorst, M. Feuerstein, and N. Navab. Advanced medical displays: A literature review of augmented reality. *Journal of Display Technology*, 4(4):451–467, 2008.

[26] N. Tai and M. Inanici. Luminance contrast as depth cue: investigation and design applications. *Computer-Aided Design and Applications*, 9(5):691–705, 2012.

[27] R. Wang, Z. Geng, Z. Zang, and R. Pei. Visualization techniques for augmented reality in endoscopic surgery. *Medical Imaging and Augmented Reality*, 2016.

[28] I. Wolf, M. Vetter, I. Wegner, M. Nolden, T. Böttger, M. Hastenteufel, M. Schöbinger, T. Kunert, and H.-P. Meinzer. The medical imaging interaction toolkit (MITK). *http://www.mitk.org/*.

[29] S. Zollmann, D. Kalkofen, E. Mendez, and G. Reitmayr. Image-based ghostings for single layer occlusions in augmented reality. *International Symposium on Mixed and Augmented Reality*, 2010.